Structural Simulation of Wheelchair Ramp using Finite Element Method

Bhre Wangsa Lenggana[1*], Agung Nugroho[2], Ubaidillah[2]

[1]*Department of Mechanical Engineering, Universitas Jenderal Soedirman, Purwokerto, 53122, Indonesia*
[2]*Department of Mechanical Engineering, Universitas Sebelas Maret, Surakarta, 57126, Indonesia*
**Corresponding author:bhre.lenggana@unsoed.ac.id*

Article history:
Received: 23 August 2024 / Received in revised form: 6 September 2024 / Accepted: 26 September 2024
Available online 16 October 2024

ABSTRACT

Wheelchairs are essential mobility aids for people with disabilities, but they are often limited to flat surfaces and cannot overcome height differences. Portable ramps are an effective solution to overcome this limitation. This research aims to simulate and analyze the structure of a portable ramp for wheelchairs. Simulations were conducted using finite element method analysis software to assess the portable ramp's von Mises stress, deformation, and safety factor in various loading positions. Finite element method (FEM) analysis software was utilized to evaluate key mechanical properties, including von Mises stress, deformation, and safety factor, under different loading conditions and positions. The simulation results demonstrated that the proposed portable ramp design can safely endure various load placements without exceeding the material's stress limits. The von Mises stress, deformation, and safety factors remained within acceptable ranges, validating the ramp's structural integrity and safety. Based on the initial findings, design modifications were implemented to further enhance the ramp's strength, durability, and user safety. This research not only confirms the effectiveness of the proposed ramp but also suggests improvements to optimize its performance. The final portable ramp design offers a reliable, cost-effective, and market-competitive solution that can significantly improve the mobility and independence of wheelchair users, enabling them to navigate a broader range of environments and overcome everyday obstacles with greater ease and confidence.

Keywords: *Deformation, finite element, portable ramp, safety factor, von Mises*

I. Introduction

Wheelchairs are an alternative means of fulfilling the activity needs of people with disabilities to increase activity independence. This is because most people with disabilities have limitations in moving, so a wheelchair is needed which acts as a transportation aid. The use of wheelchairs is the most effective tool for people with disabilities in overcoming mobility barriers [1]. On the other hand, wheelchairs can also be used as a place of rehabilitation for disabled limbs, thereby improving the quality of life and health levels for people with disabilities [2]. Wheelchair mobility is still limited, such as the limitations of moving places with certain surface height differences. Therefore, there is a need for assistive devices to improve wheelchair mobility such as the use of ramps. The ramp is one of the devices to improve wheelchair accessibility by overcoming small height differences, both in urban areas and inside buildings. Ramps can connect walkways or stepped concourses at different levels [3]. However, the ramps often used around are still in the form of ramps that cannot be moved, so a ramp with a portable type is needed to increase wheelchair mobility. The portable ramp allows wheelchairs to be used in various conditions.

DOI: 10.17977/um016v8i22024p306

The safety of the ramp design on the car can be seen based on the shape and condition of the structure after loading. The shape of the ramp can be determined by design selection and weighting to meet accessibility and safety needs. On the other hand, the safety of ramp design based on structural conditions can be seen from von Mises stress, deformation, and safety factors. The use of von Mises stress value as the basis of ramp design safety is because the value can define structural failure by knowing the point that experiences maximum stress. The maximum stress value can determine the deformation value that occurs so that calculations can be made to determine the safety factor in the portable ramp design.

One way that can be used to analyze portable ramps based on structural conditions is by using the finite element method approach. The analysis considers the loading mass at various points on the portable ramp. This is done because the position of the load on the portable ramp changes. Suppose the resulting values of von Mises stress, deformation, and safety factor exceed the limit of safe conditions. In that case, some geometric changes can be applied in the design to be safe when used [4]. Considering the safety of ramp design is very influential on the performance of ramp structure conditions, especially its effect on von Mises stress, deformation, and safety factor. However, there are still very few studies that discuss portable ramps for cars. Thus, this study was conducted to determine the effect of design selection and structural conditions after portable ramp loading on the safety of ramp design in cars, focusing on variations in loading position. Overall, this research can spur the future development and implementation of portable ramps.

Research conducted by Storr et al. (2004) [5] describes portable ramp lengths that vary between 2 to 3 meters. The choice of this size was based on the fact that a portable ramp of this length would not exceed the maximum gradient of 1:4 recommended by powered wheelchair providers when used with vehicles that have a floor height of approximately 56 cm. This average floor height was obtained from measurements on a sample of 10 estate cars and people carriers. According to Nur et al. (2023) [6], ramp profile is a crucial aspect as it can affect potential damage to the vehicle and driving comfort. Factors such as slope, gradient, minimum width, ramp geometry design, and ramp length are described as critical elements in considering the influence of ramp design. In addition, another factor that directly affects the ramp is design consistency. In addition, according to Wang and Wei (2020) [7] to understand the ramp view is by grouping corner projections, ramp vanishing points, estimating the ramp plane, and slope. This method extracts edge lines based on geometric inference.

According to Ahamed et al. (2022) [8], the design of stair ramps has a major focus on developing designs and conducting 3D analysis with various loads and working conditions. The design process is carried out by considering the analysis as well as ensuring that the staircase meets three critical requirements: economic feasibility, technical feasibility, and social acceptability. Through this study, we are encouraged to re-examine architectural elements from a new perspective, as well as to explore the innovative characteristics of traditional structures by utilizing cutting technology [8].

According to Taskaya et al. (2018) [9], the finite element method can be used to evaluate the maximum von Mises stress during static and dynamic loading using 3D and to determine the magnitude and distribution of equivalent stresses in various components [9]. The finite element method can be used in analyzing the deformation, mechanical, and elastic stresses of portable ramps with different loading positions [10]. This research involves important parameters in creating an optimal portable ramp design for wheelchairs. One of the important parameters in the design is to customize the mass of the portable ramp. Thus, the

creation of an optimal design can help people with disabilities [11]. Portable ramps are used by wheelchair users and provide a temporary solution to improve accessibility and mobility. In general, these ramps are expected to be compact and lightweight for easy use and storage. Various types of portable ramps on the market that can be used by wheelchair users are generally not modular (telescopic and foldable) [12].

II. Material and Methods

1. Finite Element Models

The simulation was done using the ANSYS. The model was designed using the Fusion 360. We then conduct the FEM simulation using Ansys Static Structure software. Completion of the finite element method can be done by utilizing matrices, depending on the type of element. For example, from one-dimensional lines to three-dimensional elements such as cubes, which have 8 points at each corner. Each of these points has 3 degrees of freedom, so a single cube (hexahedron) has a total of 24 degrees of freedom. A model can consist of thousands of elements, making it impractical to calculate manually. Therefore, the use of matrices and computational methods becomes essential in dealing with the complexity of finite element calculations [13]. To give the researchers a more comprehensive view, the finite element method offers a great deal of variance in the test. Through the use of the finite element method and a static structural approach, the goal of this simulation is to determine the causes of portable ramp failure. It includes simulations of deformation, stress, and safety factor [14].

2. Design Requirement and Objective

The method is used to identify the elements of value that users expect in the product, thus allowing the designer to focus on aspects that are important to users which refer to the portable ramp standard. The design requirements and objective of the study are shown in Table 1.

Table 1. Design requirements and objectives

No.	Requirements	Criteria	*Demands* (D)/*Wishes* (W)
1	Geometry	– Dimensions 2100 mm long and 210 mm wide	D
		– Weight less than 10 kg	W
		– Able to withstand loads up to a maximum of 100 Kg	D
		– Portable and foldable	D
		– Strong and rust resistant	D
2	Operation	– Can be operated by a min. 1 person to install and push the wheelchair	D
3	Production	– Using materials available in market	D
		– Minimize the use of custom parts	W
4	Material	– Using composite materials and aluminum	D
		– Standard components preferred	W
5	Safety	– Tool is safe to use to withstand the weight of an adult up to 100 Kg	D
6	Assembly	– Easy to maintain	D

In concept discovery, some of the identification used is sketching. Sketching is the process of generating creative ideas without any preliminary judgment. The designer must record all ideas without ignoring any possibilities. This stage is included in the selection of sketches to design a portable ramp tool. After developing various concept ideas, the next step is conceptualization, where the ideas are converted into more detailed and specific concepts. The designer should consider various factors such as possible technical aspects, cost, time, and other relevant matters during this process [15]. This method is used to select the concept that best fits the needs and criteria that have been predetermined. The concepts generated from the idea development stage are assessed based on certain criteria to determine the best concept. This concept selection is in accordance with the VDI 2555 standard as shown in Figure 1 [15], [16].

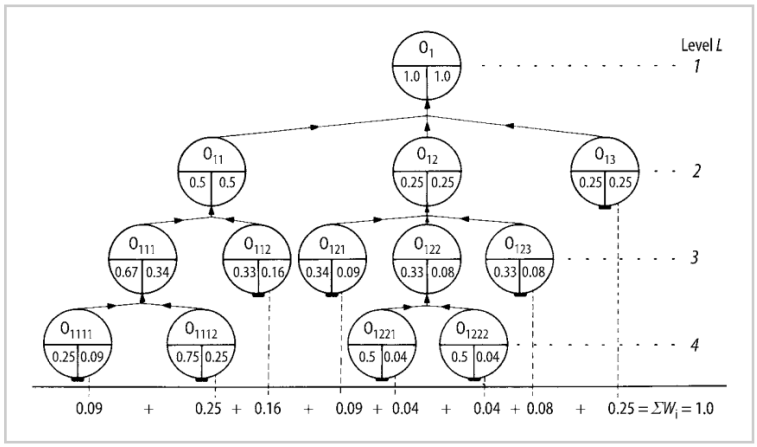

Fig. 1. Design selection weighting method [9]

3. Geometry and Meshing

Based on the first variation design in Figure 2, using a ramp base with dimensions of 1050 × 210 mm and 3 mm in thickness, a double ramp base structure is applied on the right and left sides coupled with bolted hinges.

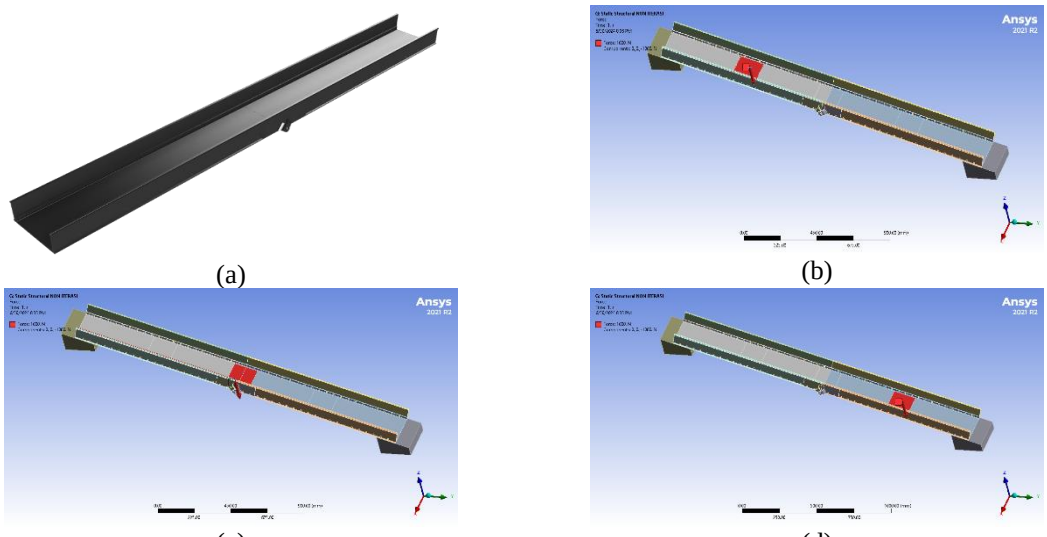

Fig. 2. Design of portable ramp (a) and loading position; (b) top; (c) middle; and (d) bottom

The loading is applied at three different points, i.e., when the top, middle and bottom are loaded at an angle of 14 degrees as shown in Figure 2. The applied load in each simulation is 1000 N. The ramp design uses a total of 76 rivets with the rivet position on the side plate that connects the side plate to the base plate. The contact between the rivet and the base plate and side plate is bonded, which means it is bound to each other between the rivet, base plate, and side plate.

As a simulation process, support in simulation conditions is given to two parts that are the support of the ramp according to real conditions. The fixed load support is placed on the part as shown in Figure 3.

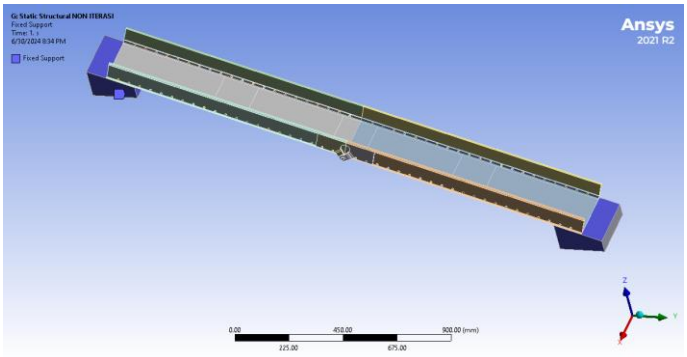

Fig. 3. Placement of fixed support in the simulation process

The element size used in the portable ramp is 8 mm to 20 mm. The smaller the element size used, the longer the computation time required. The mesh size is made with variations from 8 mm to 20 mm in increments of 1 mm to determine convergent results, where the meshing size converges at variations of 12 mm to 14 mm as shown in Figure 4. So the meshing used on the portable ramp is 12 mm with the number of nodes 191313 and the number of elements 81638.

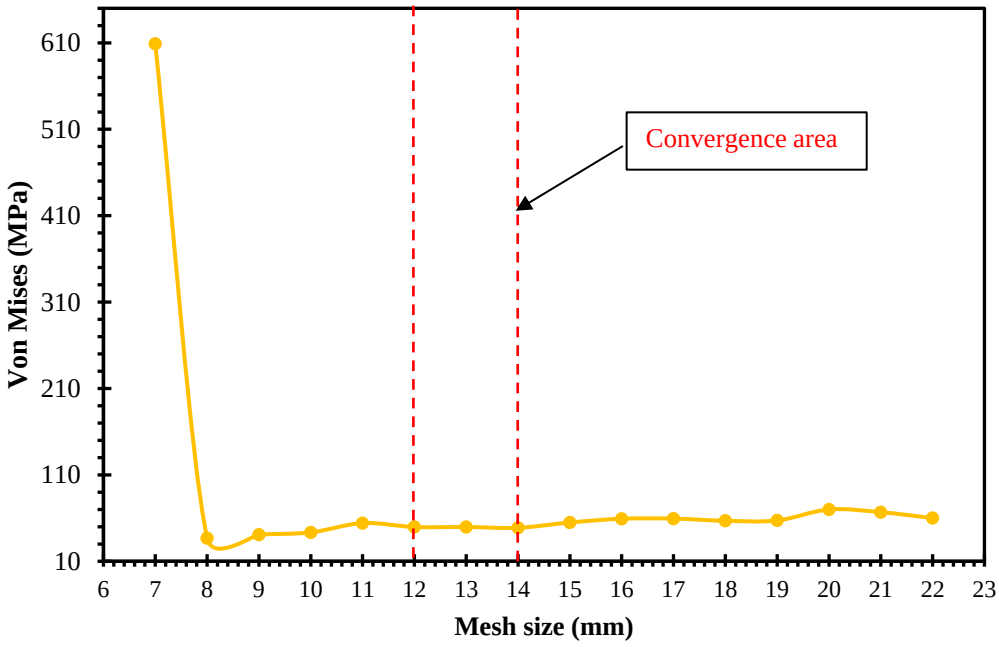

Fig. 4. Mesh convergence area

4. Materials

A macroscopic mixture of two or more different materials combined or mixed into a usable material is called a composite material [17]. Composites typically consist of a matrix that has reinforcement material inside of it. Reinforcement phases come in three different forms: fiber, flake, or particle [18]. The material used in this study is glass fiber-reinforced polymer for the base of the ramp. Glass fiber-reinforced polymer material properties were obtained from the research of Zainuddin et al. [19]. The material properties that is used in this study are shown in Table 2 below. In addition, the side of the ramp uses Aluminum 6061 material, and the bolts and rivets use steel material imported from the engineering database.

Table 2. Properties glass fiber reinforced polymer, aluminium 6061, and the structural steel material

Parameter	**Description**
Material	*Glass Fiber Reinforced Polymer*
Density	1.557 g/cm^3
Yield Strength	37.36 MPa
Ultimate Tensile Strength	95.174 MPa
Young's Modulus	2.668 GPa
Poisson's Ratio	0.33
Material	*Aluminium 6061*
Density	2.7 g/cm^3
Yield Strength	276 MPa
Ultimate Tensile Strength	310 MPa
Young's Modulus	68.9 GPa
Poisson's Ratio	0.33
Material	Structural Steel
Density	7.85 g/cm^3
Yield Strength	250 MPa
Ultimate Tensile Strength	460 MPa
Young's Modulus	200 GPa
Poisson's Ratio	0.3

III. Results and Discussions

1. Validation

The initial data collection aims to verify the results of previous research conducted by Wibawa [20]. This verification process aims to compare the maximum value of stress and deformation of the simulation results that have been carried out. The goal is to ensure the validity of the simulation. In his research, Wibawa analyzed the simulation of the strength of the AC bracket. The AC bracket frame was given static loads at 16 kg, 18 kg, 20 kg, and 22 kg. Wibawa's simulation results [20] showed a von-Mises stress of 103.699 MPa and a deformation of 1.626 mm at a load of 22 kg.

This study shows the result of von Mises stress of 100.94 MPa and deformation of 1.7272 mm. The difference between the latest simulation results and the previous simulation shows the Von-Mises stress decreased by 2.759 MPa (2.66%), and the deformation increased by 0.1012 mm (6.22%). Based on the data obtained, it shows that the difference

in simulation results meets the comparison tolerance requirement of less than 10%. This can be seen in Figures 5 and 6.

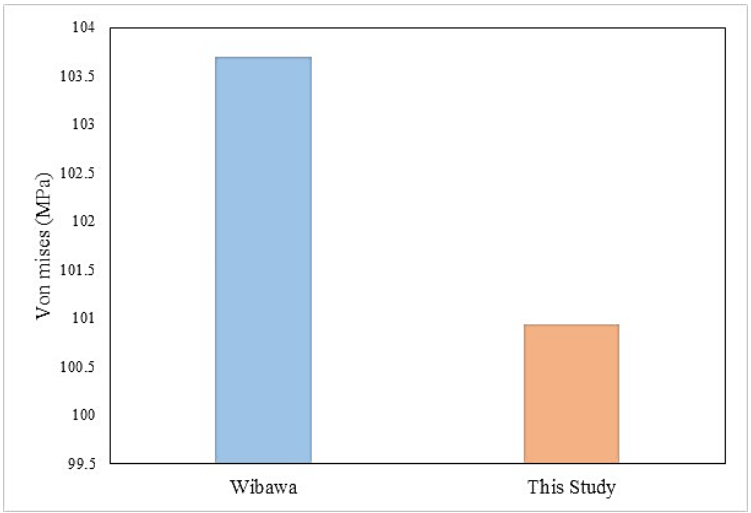

Fig. 5. Comparison of Wibawa and simulation von Mises stress results

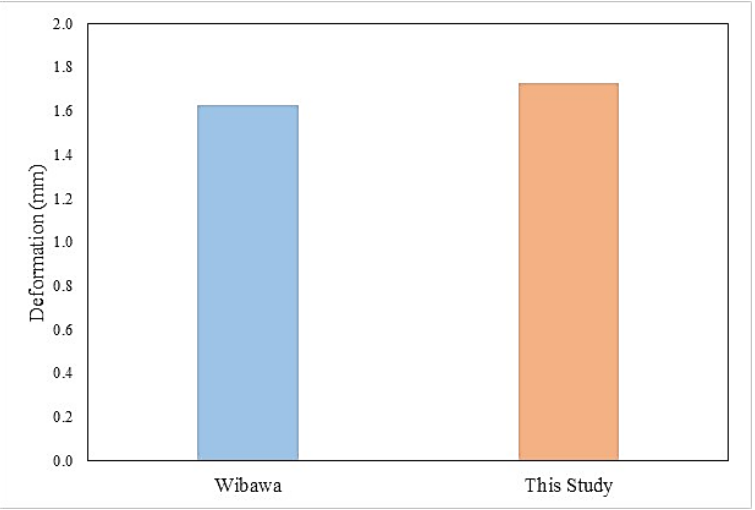

Fig. 6. Comparison of Wibawa and simulation deformation results

2. First Variation Design

The top of the ramp was subjected to a load of 1000 N resulting in a maximum recorded stress of 71.47 MPa, located at the hinge of the bolt connection, as shown in Figure 7. This situation was caused by the intersection of the ramp base with the ramp side, creating a point of high stress. Figure 8 shows a total deformation of 11.646 mm at the top center of the ramp base. This deformation occurs because the different materials used between the base of the ramp and other parts have different strengths, so that the base of the ramp experiences maximum deflection due to the applied load. The safety factor of this frame is 1.26, as shown in Figure 9.

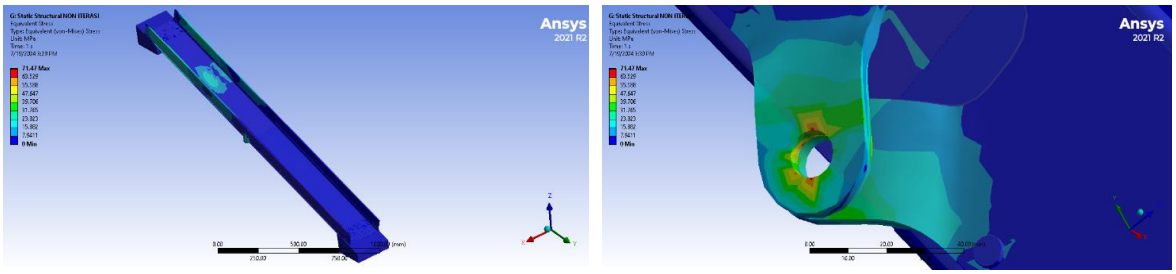

(a) (b)

Fig. 7. Von Mises stress of portable ramp top loading (a) isometric view and (b) critical point

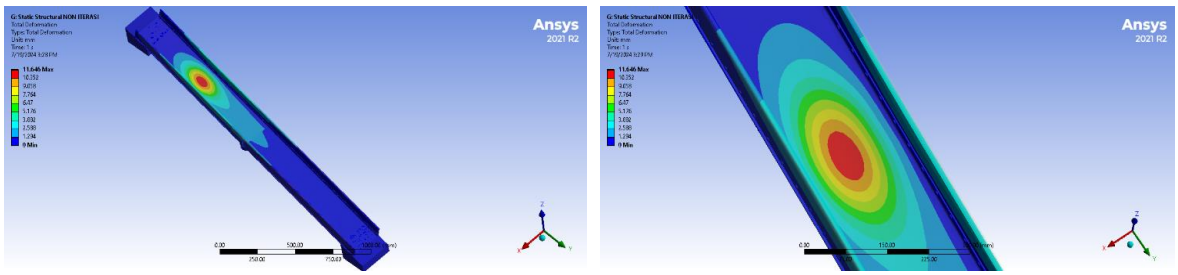

(a) (b)

Fig. 8. Deformation of portable ramp top loading (a) isometric view and (b) critical point

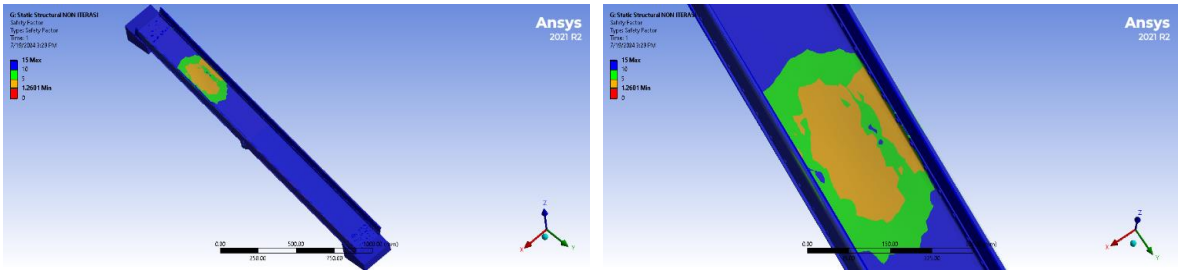

(a) (b)

Fig. 9. Safety factor portable ramp top loading (a) isometric view and (b) critical point

The middle of the ramp was subjected to a loading of 1000 N resulting in a maximum recorded stress of 79.054 MPa, occurring at the right and left hinge sections at the bolt connections, as shown in Figure 10. This is due to the hinge joining the top and bottom of the ramp creating a point of high stress. Figure 11 shows a total deformation of 18.966 mm at the middle of the ramp base. This deformation occurs because the material of the ramp base and ramp sides are different and the location is far from the upper and lower main support frames, thus experiencing the maximum deflection due to the applied load. The safety factor of this frame is 0.80, as shown in Figure 12. The safety factor on the middle plate is 0.8 below 1.0, indicating that structural failure occurred because the base material of the ramp and the side of the ramp is different and the location is far from the upper and lower main support frames, so that it experiences maximum deflection due to the applied load.

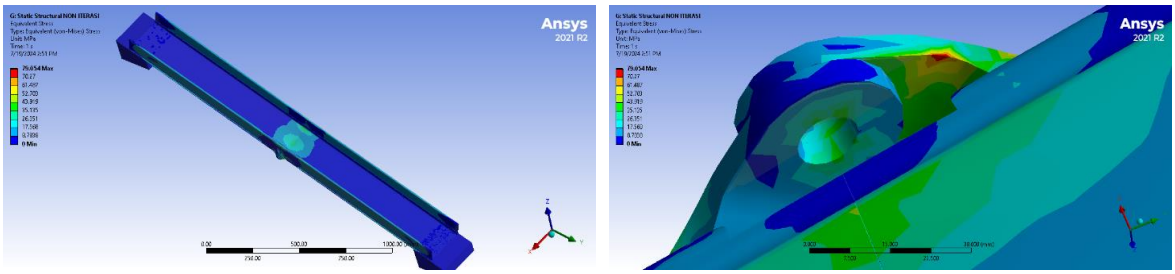

(a) (b)

Fig. 10. Von Mises stress of portable ramp loading middle section (a) isometric view and (b) critical point

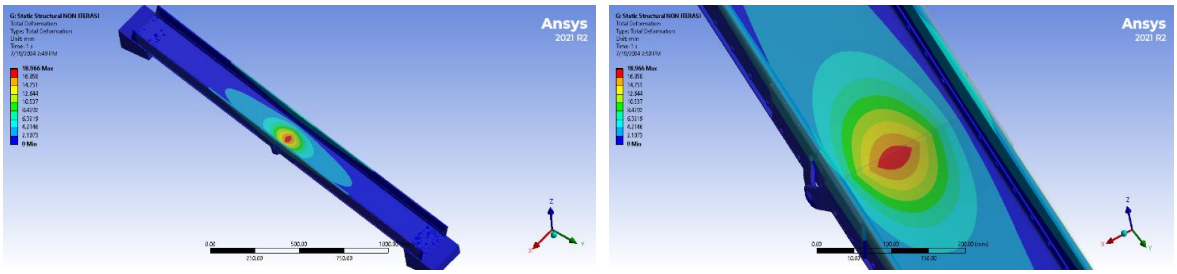

(a) (b)

Fig. 11. Deformation of portable ramp loading middle section (a) isometric view and (b) critical point

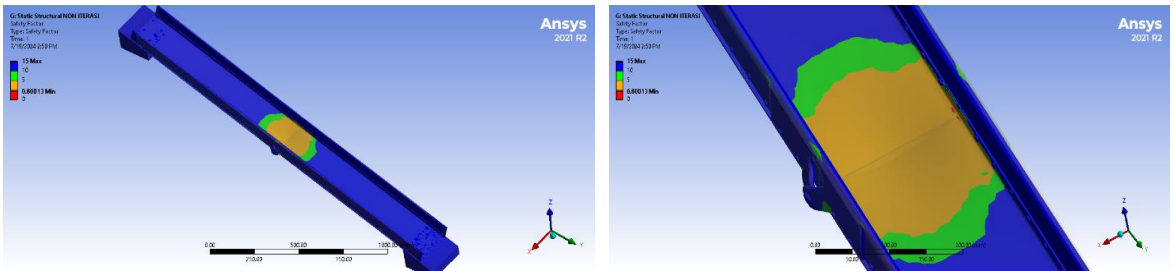

(a) (b)

Fig. 12. Safety factor of portable ramp loading middle section (a) isometric view and (b) critical point

The bottom of the ramp was subjected to a loading of 1000 N resulting in a maximum recorded stress of 65.16 MPa at the right and left hinge sections at the bolt connections, as 65.16 shown in Figure 13. This situation is caused by the intersection of the ramp base and the ramp side, creating a point of high stress. Figure 14 shows a total deformation of 11.586 mm at the top middle of the ramp base. This deformation occurs because the different materials used between the base of the ramp and other parts have different strengths, so that the base of the ramp experiences maximum deflection due to the applied load. The safety factor of this frame is 1.26, as shown in Figure 15.

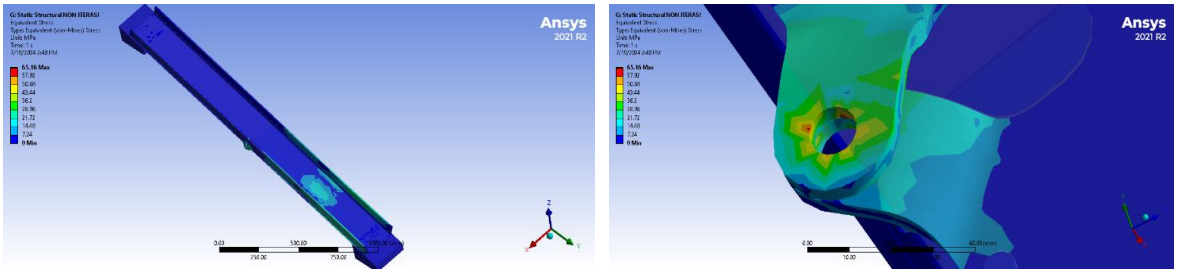

(a) (b)

Fig. 13. Von Mises stress of portable ramp bottom loading (a) isometric view and (b) critical point

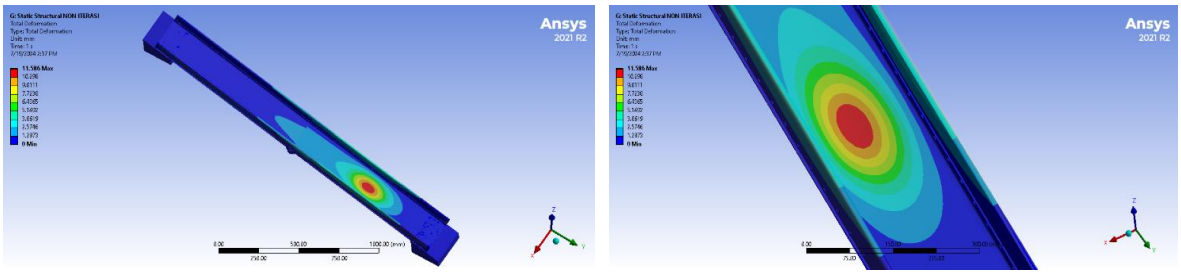

(a) (b)

Fig. 14. Deformation of portable ramp bottom loading (a) isometric view and (b) critical points

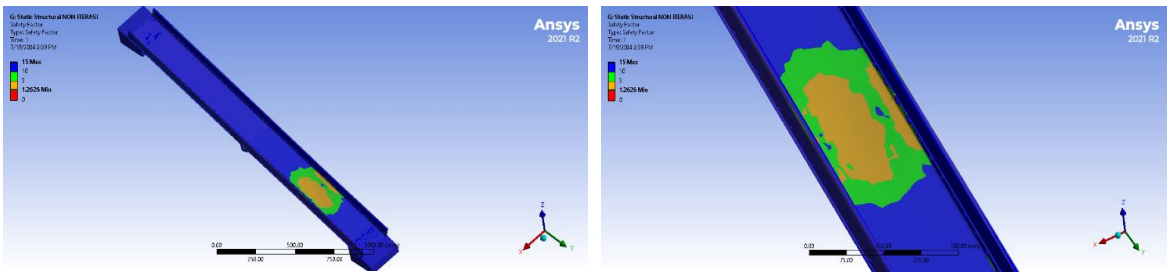

(a) (b)

Fig. 15. Safety factor portable ramp bottom loading (a) isometric view and (b) critical point

The simulation results carried out in the first variation obtained the results of the second point loading, namely a safety factor of 0.80. These results cause the portable ramp design to be said to be unsafe to use because the safety factor has a value below the minimum requirement of 1.25.

3. Second variations

This second variation design is an iteration of adding portable ramp thickness to certain areas that experience high failure. So that in the middle area above and below the base of the ramp is given an additional thickness of 340 mm long, 160 mm wide, and 2 mm thick. While in the middle of the base of the ramp that is connected to the hinge is given an additional thickness of 320 mm long, 160 mm wide, and 2 mm thick as shown in Figure 16.

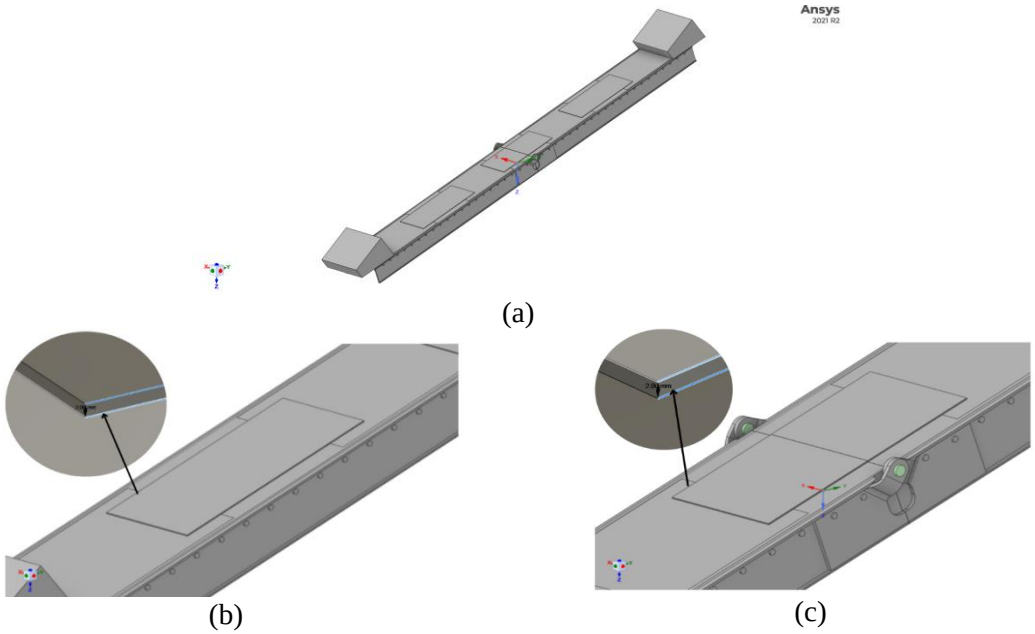

(a)

(b) (c)

Fig. 16. Second variations

The top of the ramp was loaded with 1000 N resulting in a maximum recorded stress of 45.077 MPa, located at the hinge of the bolt connection, as shown in Figure 17. This situation is caused by the meeting of the base of the ramp with the side of the ramp that intersects with each other, creating a point with high stress. The stress value in this second variation has decreased by 26.393 MPa. Figure 18 shows a total deformation of 6.27 mm at the top middle of the ramp base. This deformation occurs because the different materials used between the base of the ramp and other parts have different strengths, so that the base of the ramp experiences maximum deflection due to the load applied. The deformation value decreased by 5.376 mm. The safety factor of this frame is 1.637, as shown in Figure 19. The safety factor value has increased by 0.377.

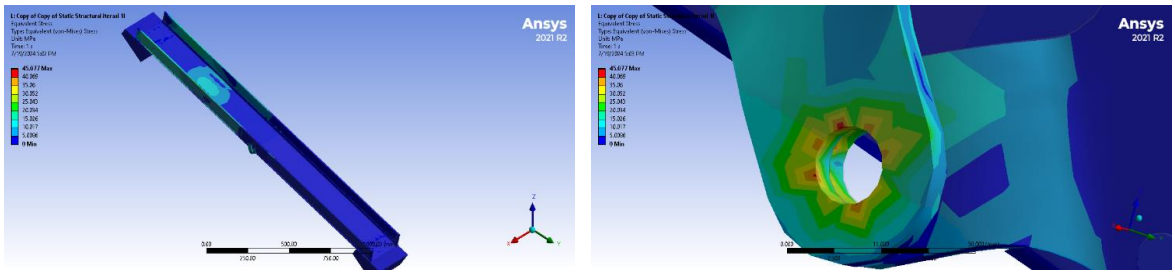

(a) (b)

Fig. 17. Portable ramp voltage top loading (a) isometric view and (b) critical point

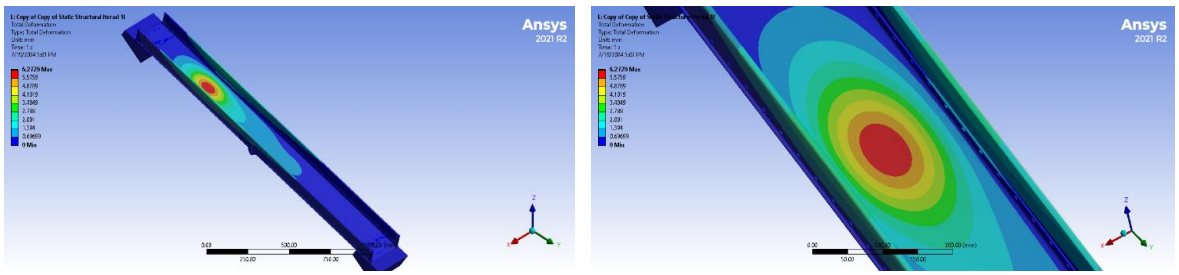

(a) (b)

Fig. 18. Deformation of portable ramp top loading (a) isometric view and (b) critical point

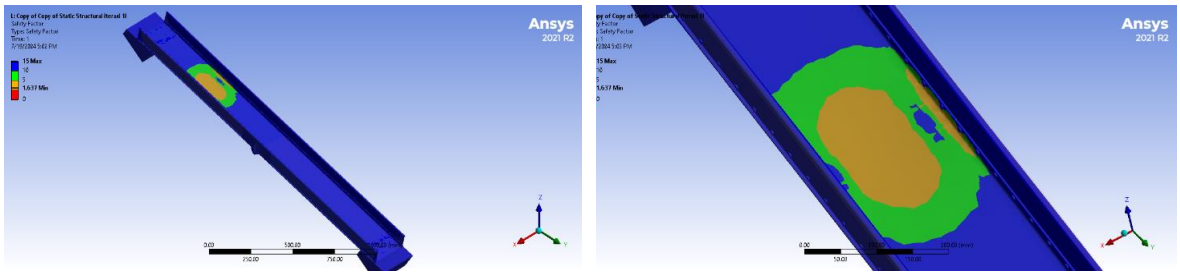

(a) (b)

Fig. 19. Safety factor portable ramp top loading (a) isometric view and (b) critical point

The middle of the ramp was subjected to a loading of 1000 N resulting in a maximum recorded stress of 47.176 MPa, occurring at the right and left hinge sections at the bolt connections, as shown in Figure 20. This situation is caused by the hinge joining the base of the upper and lower ramps creating a point of high stress. The stress value in this second variation decreased by 31.878 MPa. Figure 21 shows a total deformation of 7.05 mm at the middle of the ramp base. This deformation occurs because the material of the base of the ramp and the side of the ramp is different and the location is far from the upper and lower

main support frames, so it experiences maximum deflection due to the applied load. The deformation value decreased by 11.916 mm. The safety factor of this frame is 1.70, as shown in Figure 22. The safety factor value has increased by 0.9.

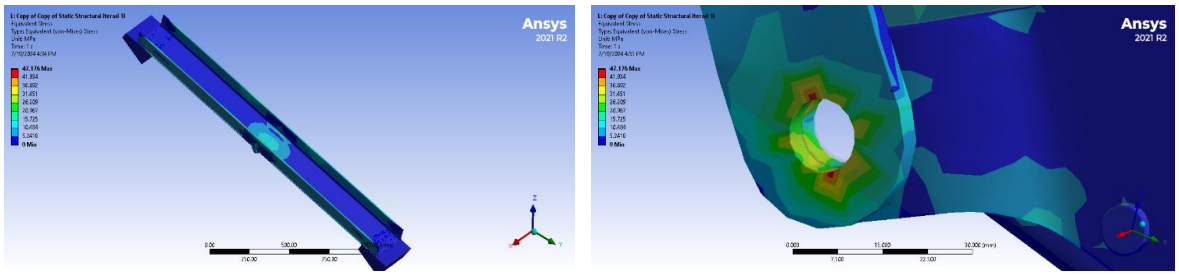

(a) (b)

Fig. 20. Portable ramp stress loading middle section (a) isometric view and (b) critical point

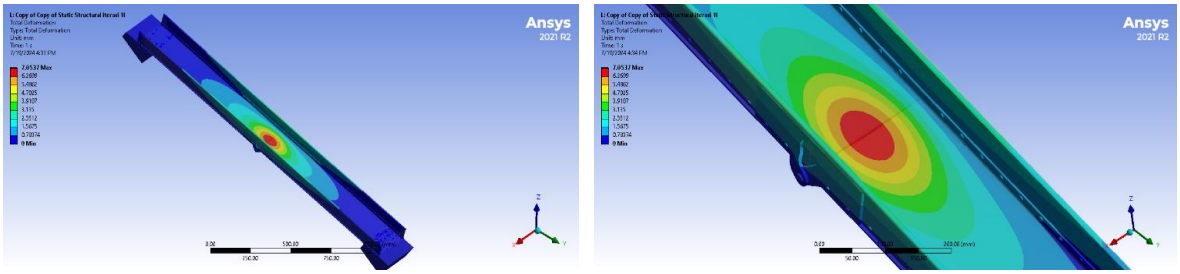

(a) (b)

Fig. 21. Deformation of portable ramp loading middle section (a) isometric view and (b) critical point

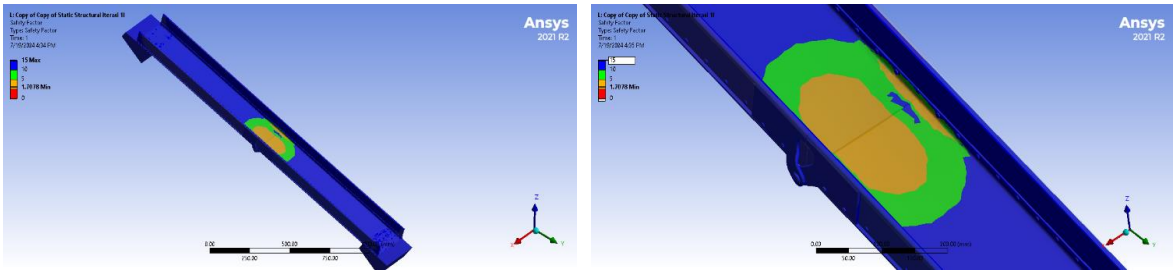

(a) (b)

Fig. 22. Safety factor portable ramp loading middle section (a) isometric view and (b) critical point

The bottom of the ramp was subjected to a loading of 1000 N resulting in a maximum recorded stress of 51.45 MPa at the right and left hinge at the bolt connection, as shown in Figure 23. This situation is caused by the meeting of the bottom of the ramp with the side of the ramp that intersects with each other, creating a point with high stress. The stress value in this second variation decreased by 13.71 MPa. Figure 24 shows a total deformation of 6.27 mm at the top center of the ramp base. This deformation occurs because the different materials used between the base of the ramp and other parts have different strengths, so that the base of the ramp experiences maximum deflection due to the applied load. The deformation value decreased by 5.316 mm. The safety factor of this frame is 1.64, as shown in Figure 25. The safety factor value has increased by 0.38.

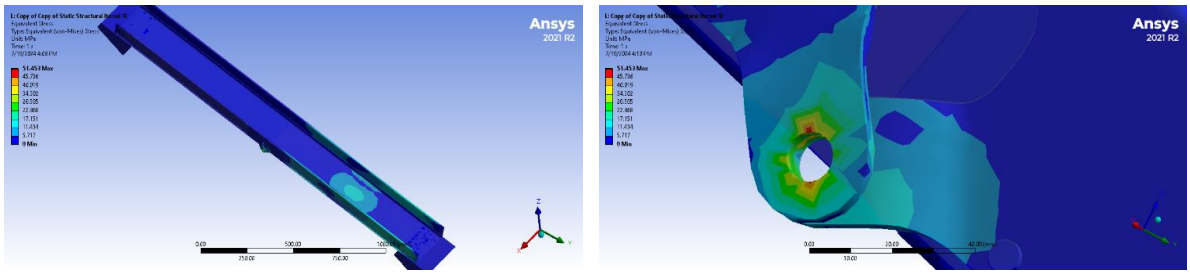

(a) (b)

Fig. 23. Portable ramp bottom loading stress (a) isometric view and (b) critical point

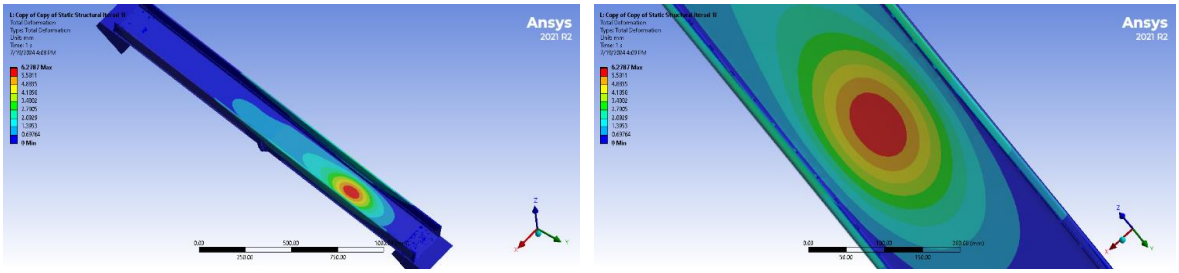

(a) (b)

Fig. 24. Deformation of portable ramp bottom loading (a) isometric view and (b) critical points

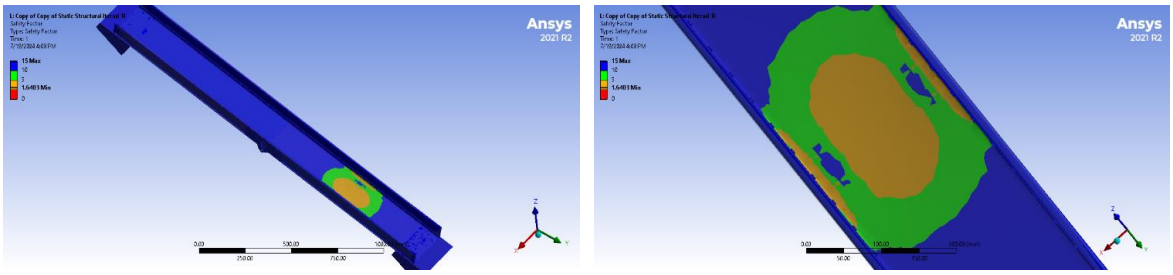

(a) (b)

Fig. 25. Safety factor portable ramp bottom loading (a) isometric view and (b) critical point

4. Variation analysis results

The stress, deformation, and safety factor on the frame are calculated based on the colour code shown in the figure. In the first variation of the top loading, a stress of 71.47 MPa, a deformation of 11.646 mm, and a safety factor of 1.26 were found. Then the middle loading found a stress of 79.054 MPa, a deformation of 18.966 mm, and a safety factor of 0.80. The last loading result at the bottom found a stress of 65.16 MPa, a deformation of 11.586 mm, and a safety factor of 1.26. The simulation results show that even though the portable ramp is not strong enough to withstand the given load due to the safety factor value which is still below 1.25. So it is required to do the second variation. In the second variation with the addition of thickness at the base of the ramp in the part that experienced the highest change, at the top loading, the stress increased to 45.077 MPa with a deformation of 6.27 mm, and the safety factor remained 1.637. Then the middle loading found a stress of 47.176 MPa, a deformation of 7.05 mm, and a safety factor of 1.70. The last loading at the bottom found a stress of 51.453 MPa, a deformation of 6.27 mm, and a safety factor of 1.64.

In static loading analysis, stress, deformation, safety factor, and mass are the main criteria to evaluate the design advantages. Simulations show that by adding thickness to the basic structure of the ramp, there is an increase in the safety factor acting on the portable

ramp and a decrease in the von mises stress and deformation acting on the portable ramp. This is due to the decrease in the number of frame members, which results in a smaller distribution of forces received by each member. The results of the von mises stress comparison between the first variation design and the second variation can be seen in Figure 26 below. The results of the deformation comparison between the first variation design and the second variation can be seen in Figure 27 and the results of the safety factor comparison between the first variation design and the second variation can be seen in Figure 28.

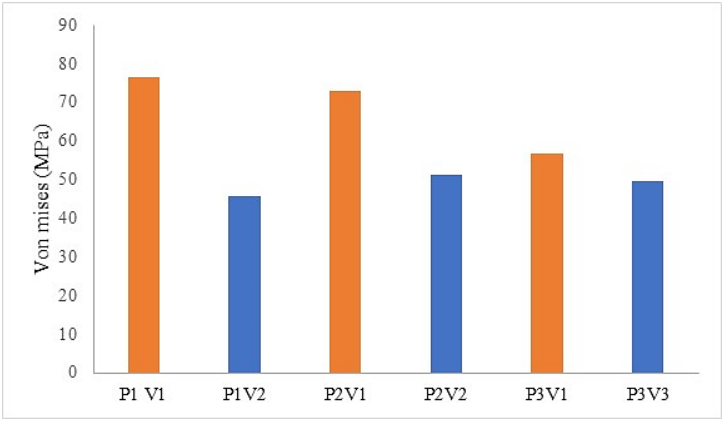

Fig. 26. Comparison of von Mises stress

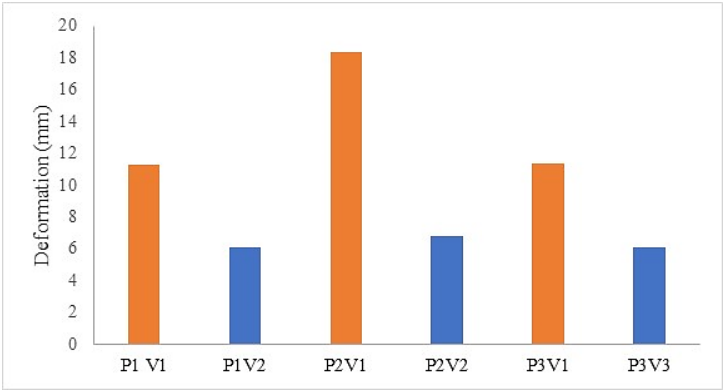

Fig. 27. Comparison of deformations

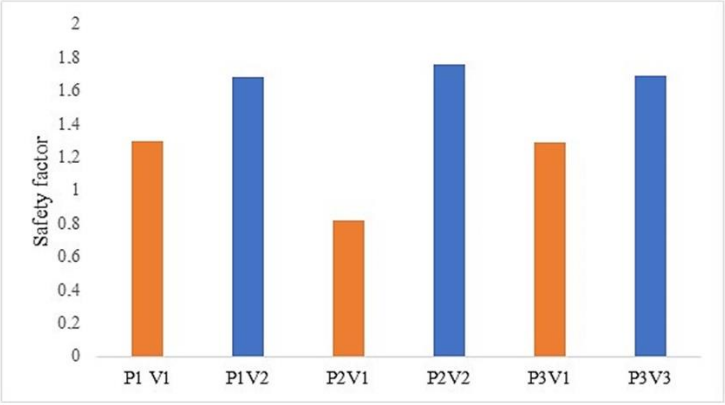

Fig. 28. Comparison of safety factors

IV. Conclusions

Research on the manufacture and selection of ramp designs which are then simulated using the finite element method with Ansys Workbench Static Structure software. Based on the test data, there are several conclusions. The results of the analysis show that varying load positions affect the von mises stress values on the portable ramp. The first variation design has the highest stress at the top of 79.054 MPa. The second variation design that has experienced additional thickness in certain parts shows that the bottom loading has the highest stress of 51.453 MPa. The maximum stress occurs at the hinge section which is the critical point in the design. This highlights the importance of analyzing the load position in ensuring the structural safety of the portable ramp. Deformation analysis shows that the portable ramp can maintain deformation within safe limits even with varying load positions. The first variation design experienced the highest deformation at the center loading of 18.966 mm and the second variation design experienced the highest deformation at the center loading of 7.05 mm. The measured deformations are below the acceptable threshold, thus ensuring that the portable ramp remains comfortable and safe to use in various conditions. Calculation of safety factor based on von mises stress and deformation shows that the portable ramp design has adequate safety factor. The first variation design has the smallest safety factor of 0.80 when loading the center. The second variation design has the lowest safety factor of 1.637 at the top loading. The resulting safety factor ensures that the portable ramp can be used safely under various loading conditions without the risk of structural failure. Therefore, this research successfully achieved its objectives and made a significant contribution to the design and analysis of portable ramps. The results of this research are expected to serve as a reference for further development and implementation of safe and efficient portable ramps.

References

[1] Q. Du, Y. Li, and L. Pan, "Wheelchair size and material application in human-machine system model", *Applied Mathematics and Nonlinear Sciences*, vol. 6, no. 2, pp. 7–18, 2021, doi: 10.2478/amns.2021.1.00009

[2] A. Syakura, S. Nurhosifah, and W.R. Yuliana, "Indonesia pengembangan kursi roda yang efektif dalam menurunkan dampak negatif imobilisasi lama pada penyandang disabilitas fisik dengan kelumpuhan: Sistematis review", *Professional Health Journal*, vol. 3, no. 1, pp. 1–8, 2021, doi: 10.54832/phj.v3i1.168

[3] V. Tatano and R. Revellini, "An alternative system to improve accessibility for wheelchair users: The stepped ramp", *Applied Ergonomics*, vol. 108. 2023, doi: 10.1016/j.apergo.2022.103938

[4] J. Singh, "Static structural analysis of suspension arm using finite element method", *Int. J. Res. Eng. Technol*., vol. 4, no. 7, pp. 402-406, July, 2015, doi: 10.15623/ijret.2015.0407064

[5] T. Storr, J. Spicer, P. Frost, S. Attfield, C.D. Ward, and L.L. Pinnington, "Design features of portable wheelchair ramps and their implications for curb and vehicle access", *Journal of Rehabilitation Research and Development*, vol. 41, pp. 443–452, 2004, doi: 10.1682/JRRD.2003.06.0091

[6] S. Nur, S. Mohd, N. Ulang, "Factor that contributes to the ramp design and the effective gradient for ramp at entrance carporch area for housing sector in double-storey house to accommodate low-clearance vehicles", vol. 1, no. 1, pp. 22–36, 2023, doi: 10.37934/aram.110.1.2236

[7] L. Wang and H. Wei, "Understanding of wheelchair ramp scenes for disabled people with visual impairments", *Engineering Applications of Artificial Intelligence*, vol. 90, 2020, doi: https://doi.org/10.1016/j.engappai.2020.103569
[8] P.U. Ahamed, K.A. Kirubakaran, B.A. Kumar, F.A. Azeez, R. Gunaseelan, and P.A. Erwin, "Design and analysis of stairs to ramp combined lifter by using 3D modelling software", *AIP Conf. Proceedings*, vol. 2385, No. 1, 2022, doi: 10.1063/5.0070813
[9] S. Taskaya, "Investigation of static structure effect according to axial coordinates by using finite element method in ansys workbench software of AISI 310 austenitic stainless cylindrical model steel," *Int. J. Sci. Eng. Sci*., vol. 2, pp. 65–70, 2018, doi:10.5281/zenodo.2538535
[10] N. Djebbar, B. Seriera, and B.B. Bouiadjra, "Finite element analysis in static and dynamic behaviors of dental prosthesis", *Struct. Eng. Mech*., vol. 55, pp. 65–78, 2015, doi: 10.12989/sem.2015.55.1.065
[11] D.E. Kumtepe, E. Çorbacıoğlu, A.N. Başoğlu, T.U. Daim, and A. Shaygan, "Design based exploration of medical system adoption: Case of wheelchair ramps", *Technology in Society*, vol. 6, no. 101620, March, 2021, doi: 10.1016/j.techsoc.2021.101620
[12] E.D. Kumtepe, A.N. Başoğlu, E. Corbacioglu, T.U. Daim, and A.A. Shaygan, "Smart mass customization design tool: a case study of a portable ramp for wheelchair users", *Health and Technology*, vol. 10, no. 3, pp. 723–737, 2020, doi: 10.1007/s12553-019-00400-w
[13] N.A. Sutisna, and M. Nabildan, "Design analysis of a tubular chassis for an electric vehicle using finite element method", *Journal of Mechanical Engineering and Mechatronics*, vol. 8, no. 1, pp. 37–51, 2023, doi: 10.33021/jtmm.v8i1.4358
[14] R. Prasetya, A. Andoko, and S. Suprayitno, "Camshaft failure simulation with static structural approach", *Journal of Mechanical Engineering Science and Technology*, vol. 5, no. 1, pp. 47–61, 2021, doi: 10.17977/um016v5i12021p047
[15] G. Pahl, W. Beitz, J. Feldhusen, and K.H. Grote, "Engineering design: A systematic approach", *Eng. Des. A. Syst. Approach*, 1–617, 2007, doi:10.1007/978-1-84628-319-2.
[16] R.N. Amrullah, S. Hadi, and M.A. Rizza, "Simulation-based methodology to investigate the impact of material type and compressive speed variation on effective strain rate and springback", *Journal of Mechanical Engineering Science and Technology*, vol. 8, no. 2, pp. 229-239, 2024, doi: 10.17977/um016v8i22024p229
[17] A. Andoko, P. Puspitasari, and A. Permanasari, "Analysis of strength of glass fibre composite leaf spring using finite element method", *Journal of Mechanical Engineering Science and Technology*, vol. 1, no. 1, pp 1–8, 2017, doi: https://doi.org/10.17977/um016v1i12017p001
[18] S. Sumarji, N.F. Albajili, M. Darsin, R.R. Sakura, and A. Sanata, 'Effect of variation of SiC mass fraction on mechanical properties of Al-SiC composite using stir casting method', *Journal of Mechanical Engineering Science and Technology*, vol. 6, no. 1, 2022, pp. 23-33, doi: 10.17977/um016v6i12022p023
[19] M. Zainudin, K. Diharjo, M. Kaavessina, D. Setyanto, and U. Ubaidillah, "Industrial implementation of aluminum trihydrate-fiber composition for fire resistance and mechanical properties in glass-fiber-reinforced polymer roofs", *Polymers*, vol. 14, no. 7, 2022, doi: https://doi.org/10.3390/polym14071273
[20] L.A.N. Wibawa, 'Desain dan analisis kekuatan dudukan (bracket) ac outdoor menggunakan metode elemen hingga', *Jurnal Crankshaft*, vol. 2, no. 1, pp. 19–24, 2019, doi: 10.24176/crankshaft.v2i1.2688